Stabilities of Ion/Radical Adducts in the Liquid Phase as Derived from the Dependence of Electrochemical Cleavage Reactivities upon Solvent

Laurence Pause, Marc Robert, and Jean-Michel Savéant*

Contribution from the Laboratoire d'Electrochimie Moléculaire, Unité Mixte de Recherche Université − CNRS No 7591, Université de Paris 7 − Denis Diderot, 2 place Jussieu, 75251 Paris Cedex 05, France

Received July 23, 2001

Abstract: The idea that significant ion/radical interactions should vary with solvent if they do exist in the liquid phase was pursued by an investigation of the dissociative electron-transfer reactivity of carbon tetrachloride and 4-cyanobenzyl chloride in four different solvents, 1,2-dichloroethane, *N*,*N*-dimethylformamide, ethanol, and formamide, by means of their cyclic voltammetric responses. Modification of the conventional dissociative electron transfer theory to take account of an interaction between fragments in the ion/radical pair resulting from the dissociative electron reaction allows a satisfactory fitting of the experimental data leading to the determination of the interaction energy. There is an approximate correlation between the interaction energies in the ion/radical pair and the solvation free energies of the leaving anion, Cl^-. The interaction is maximal in 1,2-dichloroethane, which is both the least polar and the least able to solvate Cl^-. The interaction is smaller in the polar solvents, albeit distinctly measurable. The two protic solvents, ethanol and formamide, which are the most able to solvate Cl^-, give rise to similar interaction energies. The interaction is definitely stronger in *N*,*N*-dimethylformamide, which has a lesser ability to solvate Cl^- than the two other polar solvents. The existence of significant ion/radical interactions in polar media is thus confirmed and a route to their determination opened.

An ion and a radical are the products of the one-electron reductive or oxidative cleavage of neutral molecules, whether the cleavage follows a concerted or a stepwise pathway (Scheme 1) and regardless of the mode of injection or removal of the electron, thermal (electrochemical or homogeneous) or photoinduced.[1−9] There is preliminary experimental[10a−c] and theoretical[1a,10,11] evidence that interactions between the ion and the radical may influence considerably the reactivity patterns of reductive or oxidative cleavages. Consideration of these interactions is thus expected to be a helpful contribution to the general understanding of the dynamics of electron transfer/bond breaking processes. Conversely, careful analysis of the rate data for such reactions should provide evidence for the existence of such

Scheme 1

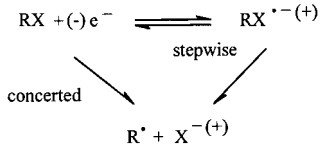

(1) (a) Savéant, J.-M. Electron Transfer, Bond Breaking and Bond Formation. In *Advances in Physical Organic Chemistry*; Tidwell, T. T., Ed.; Academic Press: New York, 2000; Vol. 35, pp 117−192. (b) Hush, N. S. *J. Electroanal. Chem.* **1999**, *470*, 170. (c) Maletin, Y. A.; Cannon, R. D. *Theor. Exp. Chem.* **1998**, *34*, 7. (d) Lund, H.; Daasbjerg, K.; Lund, T.; Occhialini, D.; Pedersen, S. U. *Acta Chem. Scand.* **1997**, *51*, 135. (e) Lund, H.; Daasbjerg, K.; Lund, T.; Pedersen, S. U. *Acc. Chem. Res.* **1995**, *28*, 313. (f) Savéant, J.-M. Dissociative Electron Transfer. In *Advances in Electron-Transfer Chemistry*; Mariano, P. S., Ed.; JAI Press: New York, 1994; Vol. 4, pp 53−116. (g) Savéant, J.-M. *Acc. Chem. Res.* **1993**, *26*, 455. (h) Savéant, J.-M. Single Electron Transfer and Nucleophilic Substitution. In *Advances in Physical Organic Chemistry*; Bethel, D., Ed.; Academic Press: New York, 1990; Vol. 26, pp 1−130.

(2) (a) Andrieux, C. P.; Le Gorande, A.; Savéant, J.-M. *J. Am. Chem. Soc.* **1992**, *114*, 6892. (b) Andrieux, C. P.; Differding, E.; Robert, M.; Savéant, J.-M. *J. Am. Chem. Soc.* **1993**, *115*, 6592. (c) Andrieux, C. P.; Robert, M.; Saeva, F. D.; Savéant, J.-M. *J. Am. Chem. Soc.* **1994**, *116*, 7864. (d) Andrieux, C. P.; Tallec, A.; Tardivel, R.; Savéant, J.-M.; Tardy, C. *J. Am. Chem. Soc.* **1997**, *119*, 2420.

(3) (a) Workentin, M. S.; Maran, F.; Wayner, D. D. M. *J. Am. Chem. Soc.* **1995**, *117*, 2120. (b) Andersen, M. L.; Mathivanan, N.; Wayner, D. D. M. *J. Am. Chem. Soc.* **1996**, *118*, 4871. (c) Antonello, S.; Musumeci, M.; Wayner, D. D. M.; Maran, F. *J. Am. Chem. Soc.* **1997**, *119*, 9541. (d) Antonello, S.; Maran, F. *J. Am. Chem. Soc.* **1997**, *119*, 12595. (e) Andersen, M. L.; Long, W.; Wayner, D. D. M. *J. Am. Chem. Soc.* **1997**, *119*, 6590. (f) Antonello, S.; Maran, F. *J. Am. Chem. Soc.* **1998**, *120*, 5713. (e) Workentin, M. S.; Donkers, R. L. *J. Am. Chem. Soc.* **1998**, *120*, 2664.

(4) (a) Maslak, P.; Guthrie, R. D. *J. Am. Chem. Soc.* **1986**, *108*, 2628. (b) Maslak, P.; Guthrie, R. D. *J. Am. Chem. Soc.* **1986**, *108*, 2637. (c) Maslak, P.; Asel, S. L. *J. Am. Chem. Soc.* **1988**, *110*, 8260. (d) Maslak, P.; Narvaez, J. N. *J. Chem. Soc., Chem. Commun.* **1989**, *110*, 138. (e) Maslak, P.; Chapmann, W. H. *J. Chem. Soc., Chem. Commun.* **1989**, *110*, 1809. (f) Maslak, P.; Narvaez, J. N. *Angew. Chem., Int. Ed. Engl.* **1990**, *29*, 283. (g) Maslak, P.; Chapmann, W. H. *Tetrahedron* **1990**, *46*, 2715. (h) Maslak, P.; Chapmann, W. H. *J. Org. Chem.* **1990**, *55*, 6334. (i) Maslak, P.; Kula, J.; Chateauneuf, J. E. *J. Am. Chem. Soc.* **1991**, *113*, 2304. (j) Maslak, P.; Kula, J. *Mol. Cryst. Liq. Cryst.* **1991**, *194*, 293. (k) Vallombroso, T. M.; Chapmann, W. H.; Narvaez, J. N. *Angew. Chem., Int. Ed. Engl.* **1994**, *33*, 73. (l) Maslak, P.; Chapmann, W. H.; Vallombroso, T. M. *J. Am. Chem. Soc.* **1995**, *117*, 12373. (m) Maslak, P.; Narvaez, J. N.; Vallombroso, T. M.; Watson, B. A. *J. Am. Chem. Soc.* **1995**, *117*, 12380. (n) Maslak, P.; McGuin J. M. *J. Chem. Soc., Chem. Commun.* **1999**, 2467.

(5) (a) Andrieux, C. P.; Savéant, J.-M. *J. Electroanal. Chem.* **1986**, *205*, 43. (b) Antonello, S.; Maran, F. *J. Am. Chem. Soc.* **1997**, *119*, 12595. (c) Pause, L.; Robert, M.; Savéant, J.-M. *J. Am. Chem. Soc.* **1999**, *121*, 7158. (d) Antonello, S.; Maran, F. *J. Am. Chem. Soc.* **1999**, *121*, 9668.

(6) (a) Severin, M. G.; Farnia, E.; Vianello, E.; Arévalo, M. C. *J. Electroanal. Chem.* **1988**, *251*, 369. (b) Costentin, C.; Hapiot, P.; Médebielle, M.; Savéant, J.-M. *J. Am. Chem. Soc.* **1999**, *121*, 4451.

(7) (a) Neta, P.; Behar, D. *J. Am. Chem. Soc.* **1980**, *102*, 4798. (b) Behar, D.; Neta, P. *J. Phys. Chem.* **1981**, *85*, 690. (c) Behar, D.; Neta, P. *J. Am. Chem. Soc.* **1981**, *103*, 103. (d) Behar, D.; Neta, P. *J. Am. Chem. Soc.* **1981**, *103*, 2280. (e) Bays, J. P.; Blumer, S. T.; Baral-Tosh, S.; Behar, D.; Neta, P. *J. Am. Chem. Soc.* **1983**, *105*, 320. (f) Norris, R. K.; Barker, S. D.; Neta, P. *J. Am. Chem. Soc.* **1984**, *106*, 3140. (g) Meot-Ner, M.; Neta, P.; Norris, R. K.; Wilson, K. *J. Phys. Chem.* **1986**, *90*, 168.

10.1021/ja0117985 CCC: $20.00
Published on Web 11/08/2001

interactions and estimates of their magnitude. In this respect, the fact that small attractive interactions give rise to large kinetic effects is quite encouraging.[1a,f,g,10]

Despite some uncertainty in the early application of quantum chemical methods to this problem,[12a−c] there is little doubt that, in the gas phase, substantial attractive interactions between ions and radicals do exist.[10a,13] For example, the energy of the interaction between CCl_3• and Cl^- has been found to be on the order of 400 meV,[10a] while, for para-substituted benzyl radicals and Cl^-, it varies, with values of 200, 250, 700, and 950 meV for the series OCH_3, H, CN, and NO_2[12d] (corresponding to carbon−chlorine distances of the order of 2.5−3 Å). These interactions may be so strong as to support the notion of σ-ion radicals (or, equivalently, of three- or one-electron bonds) in the gas phase[13a] or in apolar solid matrixes.[13b,c]

One expects these interactions to decrease or even to disappear in the liquid phase, particularly in polar solvents. There are, however, consistent clues that this is not the case, even in solvents as polar as *N*,*N*-dimethylformamide (DMF) or acetonitrile, at least when the presence of electron-withdrawing groups induces a positive charge density on the radical atom center that favors its interaction with the counteranion. A first indication in this direction resulted from the comparison of the kinetics for the reductions of benzyl and 4-cyanobenzyl bromides, which both follow a concerted electron transfer/bond breaking mechanism.[2a] The cyclic voltammetric peak potential of 4-cyanobenzyl bromide is significantly more positive than the cyclic voltammetric peak potential of benzyl bromide (by 250 mV at a scan rate of 0.1 V/s). Application of the dissociative electron transfer theory[14] to these observations led to the conclusion that the bond dissociation energy increases by 0.15 eV from the first to the second compound. However, further determinations of the bond dissociation energy by independent techniques failed to detect such a substituent effect;[15] the same conclusion was also reached by means of quantum chemical estimations.[16] These observations may be interpreted by the existence of a small attractive interaction between the caged radical and ion that would be larger in the presence than in the absence of the cyano substituent, in line with its electron-withdrawing character. An even larger similar effect is observed with phenacyl chloride and bromide, as expected from the electron-withdrawing effect of the carbonyl group. Indeed, the apparent bond dissociation energies derived from cyclic voltammetry[2d] are again significantly lower than the values derived from low-pressure pyrolysis.[17]

Another piece of evidence for the existence of ion/radical attractive interactions in a polar solvent results from homogeneous electron-transfer data concerning the initiation step of the Kornblum[18] $S_{RN}1$ reactions of 2-nitropropanate ion with 4-nitrocumyl chloride and 4-nitrobenzyl chloride in acetonitrile.[6b,10c] The ion and radical interact significantly in the case of 4-nitrobenzyl chloride, with an energy of ∼100 meV, whereas they do not in the case of 4-nitrocumyl chloride, in line with steric and electronic effects.

The most recent example concerns the electrochemistry of carbon tetrachloride in DMF, pointing to a 62 meV interaction energy between CCl_3• and Cl^- in this polar solvent.[10a]

So far, the evidence for the existence of such ion/radical pairs in polar solvents is thus 2-fold. On one hand, introduction of the corresponding interaction energy into the dissociative electron transfer model allows a satisfactory fitting of experimental data in an increasing number of cases. On the other hand, significant interactions are found only with radicals where strong electron-withdrawing effects are present in line with the anticipated reinforcement of the charge/dipole attraction between the ion and the radical. Although these are valuable clues, additional evidence of the existence of such ion/radical pairs in the liquid phase as well as further assessment of the magnitude of the interaction energies are obviously welcome. This was the objective of the work reported here. The guiding idea was that if these interactions really exist, their magnitude should vary with the nature of the solvent. It seems probable that the interaction will decrease as the stabilization of the free ion by the solvent increases. Fulfillment of these expectations would provide a solid confirmation of the reality of ion/radical interactions in the liquid phase.

It is worth noting that solvent effects on reactivity are among the most difficult problem to be handle by quantum chemical approaches, hence the importance of the gathering of experimental data and of their rationalization by semiempirical models. Another example is the effect of radical ion pairing on the dynamics of photoinduced electron-transfer reactions.[19] Despite some semantic similarity and the fact that they are both mostly electrostatic in nature, the two effects are not the same: interaction between an ion and a radical in one case and interaction between an anion radical and a cation radical in the other.

Turning back to ion/radical pairs, we investigated two systems, CCl_3• and Cl^- on one hand and the 4-cyanobenzyl radical and Cl^- on the other, through the cyclic voltammetric responses obtained for the dissociative electron-transfer reduction of the parent molecules, CCl_4 and 4-cyanobenzyl chloride, respectively. Four solvents were selected, 1,2-dichloroethane (DCE), *N*,*N*-dimethylformamide (DMF), ethanol (EtOH), and formamide (FA), so as to obtain the largest possible variation of the solvation free energy of Cl^- (the free energies of transfer from water to these solvents are 0.541, 0.497, 0.207, and 0.145 eV, respectively[20]).

(8) (a) Saeva, F. D. *Top. Curr. Chem.* **1990**, *156*, 61. (b) Saeva, F. D. Intramolecular Photochemical Electron Transfer (PET)-Induced Bond Cleavage Reactions in some Sulfonium Salts Derivatives. In *Advances in Electron-Transfer Chemistry*; Mariano, P. S., Ed.; JAI Press: New York, 1994; Vol. 4, pp 1−25. (c) Gaillard, E. R.; Whitten, D. G. *Acc. Chem. Res.* **1996**, *29*, 292.

(9) (a) Arnold, B. R.; Scaiano, J. C.; McGimpsey, W. G. *J. Am. Chem. Soc.* **1992**, *114*, 9978. (b) Chen, L.; Farahat, M. S.; Gaillard, E. R.; Gan, H.; Farid, S.; Whitten, D. G. *J. Am. Chem. Soc.* **1995**, *117*, 6398. (c) Chen, L.; Farahat, M. S.; Gaillard, E. R.; Farid, S.; Whitten, D. G. *J. Photochem. Photobiol.* **1996**, *95*, 21. (d) Wang, X.; Saeva, F. D.; Kampmeier, J. A. *J. Am. Chem. Soc.* **1999**, *121*, 4364. (e) Robert, M.; Savéant, J.-M. *J. Am. Chem. Soc*. **2000**, *122*, 514. (f) Costentin, C.; Robert, M.; Savéant, J.-M. *J. Phys. Chem. A* **2000**, *104*, 7492. (g) Pause, L.; Robert, M.; Savéant, J.-M.; *ChemPhysChem* **2000**, *1*, 199.

(10) (a) Pause, L.; Robert, M.; Savéant, J.-M. *J. Am. Chem. Soc*. **2000**, *122*, 9829. (b) Pause, L.; Robert, M.; Savéant, J.-M. *J. Am. Chem. Soc*. **2001**, *123*, 4886. (c) Costentin, C.; Hapiot, P.; Médebielle, M.; Savéant, J.-M. *J. Am. Chem. Soc.* **2000**, *122*, 5623.

(11) Marcus, R. A. *Acta Chem. Scand.* **1998**, *52*, 858.

(12) (a) Benassi, R.; Bernardi, F.; Bottoni, A.; Robb, M. A.; Taddei, F. *Chem. Phys. Lett*. **1989**, *161*, 79. (b) Bertran, J.; Gallardo, I.; Moreno, M.; Savéant, J.-M. *J. Am. Chem. Soc.* **1992**, *114*, 9576. (c) Tada, T.; Yoshimura, R. *J. Am. Chem. Soc.* **1992**, *114*, 1593. (d) Costentin, C.; Robert, M.; Savéant, J.-M. Submitted.

(13) (a) Chen, E. C. M.; Albyn, K.; Dussack, L.; Wentworth, W. E. *J. Phys. Chem.* **1989**, *93*, 6827. (b) Symons, M. C. R. *Pure Appl. Chem.* **1981**, *53*, 223. (c) Symons, M. C. R. *Acta Chem. Scand*. **1997**, *51*, 123.

(14) (a) Savéant, J.-M. *J. Am. Chem. Soc.* **1987**, *109*, 6788. (b) Savéant, J.-M. *J. Am. Chem. Soc.* **1992**, *114*, 10595. (c) Andrieux, C. P.; Savéant, J.-M.; Tardy, C.; Savéant, J.-M. *J. Am. Chem. Soc.* **1998**, *120*, 4167.

(15) (a) Clark, K. B.; Wayner, D. D. M. *J. Am. Chem. Soc*. **1991**, *113*, 9363. (b) Laarhoven, L. J. J.; Born, J. G. P.; Arends, I. W.; Mulder, P. *J. Chem. Soc., Perkin Trans. 2* **1997**, 2307.

(16) Pratt, D. A.; Wright, J. S.; Ingold, K. U. *J. Am. Chem. Soc.* **1999**, *121*, 4877.

(17) Dorrestijn, E.; Hemmink, S.; Hultsmaan, G.; Monnier, L.; Van Scheppingen, W.; Mulder, P. *Eur. J. Org. Chem.* **1999**, 607.

(18) Kornblum, N. *Angew. Chem., Int. Ed. Engl.* **1975**, *14*, 734.

(19) Gould, I. R.; Farid, S. *Acc. Chem. Res.* **1996**, *29*, 522.

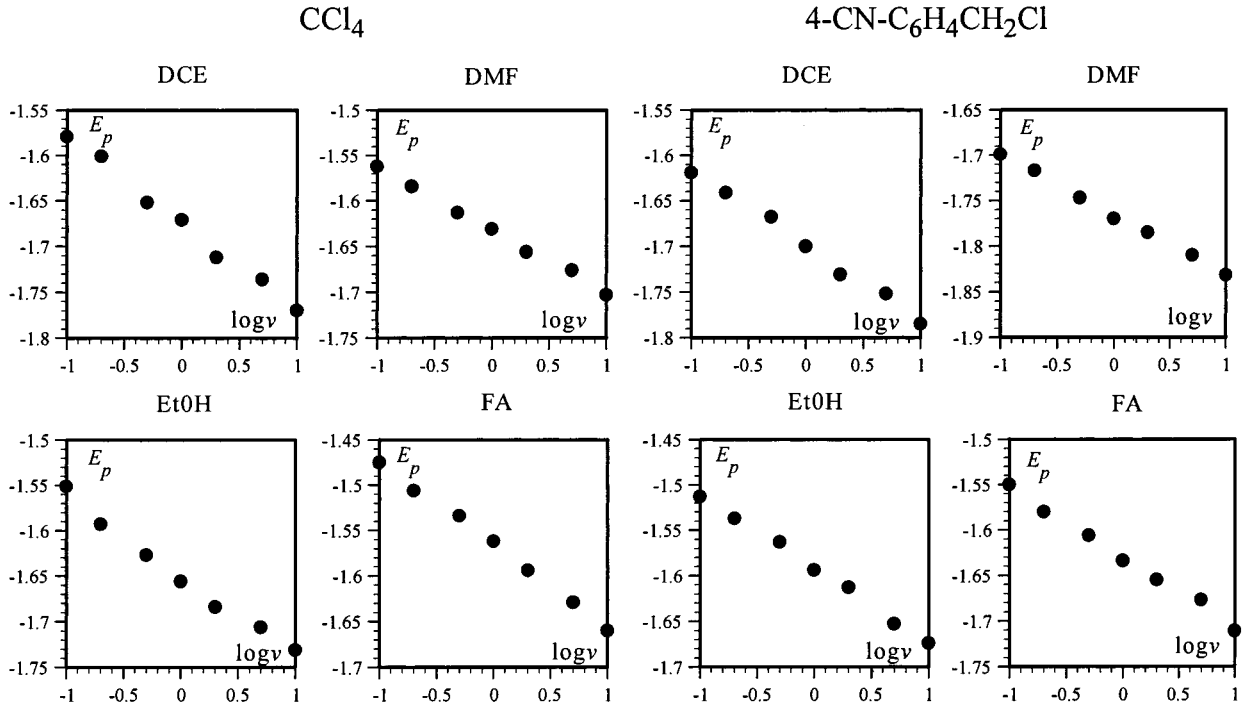

Figure 1. Peak potentials, E_p, (V vs aq SCE) corrected from ohmic drop (see Experimental Section). Supporting electrolyte: 0.1 M *n*-Bu_4BF_4. Scan rates (v) in V/s. Temperature: 20 °C.

Our strategy was as follows. Cyclic voltammetric peak potentials as a function of scan rate for the two compounds in the various solvents form the set of kinetic data on which our exploration of ion/radical pairs is based. Their treatment with an extension of the dissociative electron transfer theory that integrates the existence of an attractive interaction between the ion and the radical formed upon reductive cleavage allows the derivation of the interaction energy. The variation of the interaction energy with the solvent is then discussed with the help of an attempted correlation with the free energy of solvation of chloride ion in each solvent. The reliability of the interaction energy values and of their variation with the solvent obtained by means of this procedure requires a precise estimate of the error that may arise from potential difference between the reference electrode and the organic solution bathing the working electrode. This point will be discussed in detail. Another important parameter of the model is solvent reorganization. How the corresponding energy varies from one solvent to the other and, in each solvent, as a function of the reaction coordinate will also be scrutinized.

Results and Discussion

Cyclic Voltammetry Data. Figure 1 displays the variations of the peak potential, E_p, with the scan rate for the two compounds in all four solvents. The values of this parameter are affected by ohmic drop, especially toward the higher end of the scan rate range. Although the effect is not very big, a later hand correction is worth carrying out. This was done according to the procedure described in the Experimental Section.

Junction and Donnan Potentials between the Organic Solution and the Aqueous Reference Electrode. As emphasized earlier, the definition of a potential reference independent from the solvent is crucial to our purpose. One possibility is to select a voluminous transition metal complex as redox reference couple in the hope that solvation, being small, will be approximately the same in all solvents. This strategy suffers from serious uncertainties[21] and appears actually worse than the use of an aqueous reference electrode (i.e., saturated calomel electrode, SCE) with careful estimation of the potential difference between the organic solution and the reference electrode compartment. We may, in this connection, distinguish two cases: one when the solvent is miscible to water (all solvents but DCE) and the other when the solvent and water are immiscible (DCE). In the first case, the potential difference between the organic solution and the aqueous solution is a steady-state junction potential. In the second case, a Donnan equilibrium potential across the interface separating the two solvents must also be taken into account.

Concerning junction potentials, the classical Henderson model[22] applicable to the junction between two ionic solutions in the same solvent assumes that the concentration of each ion varies linearly from one side of the junction to the other. For extending the model to the case of two different solvents, we assume that the ionic mobilities also vary linearly across the junction from the value they have in one solvent to their value in the other solvent. Under these conditions, the difference between the potential in the organic solution, ϕ^S, and the potential of the aqueous SCE, ϕ^W, is expressed (see Supporting Information) by eq 1 (C refers to the concentration, u to the ionic mobilities, and z to the charge number).

$$\phi^S - \phi^W = -\frac{RT}{F}\sum_i \frac{|z_i|}{z_i}(C_i^S - C_i^W) \left[\frac{B}{2c}\ln\left(\frac{a+b+c}{a}\right) + \frac{A - \frac{Bb}{2c}}{\sqrt{b^2-4ac}} \ln\left(\frac{2c+b-\sqrt{b^2-4ac}}{2c+b+\sqrt{b^2-4ac}}\,\frac{b+\sqrt{b^2-4ac}}{b-\sqrt{b^2-4ac}}\right)\right] \quad (1)$$

(20) Marcus, Y. *Ion Properties*; Marcel Dekker: New York, 1997.

(21) Marcus, Y. *Pure Appl. Chem.* **1986**, *58*, 1721.

Table 1. Solvent Parameters[a]

	DCE	DMF	EtOH	FA
$\Delta^t G^{W\to S_b}_{Cl^-}$	0.541	0.497	0.207	0.145
$-G^S_{Cl^-}$ [c]	3.056	3.1	3.39	3.455
$E^\circ_{Cl^\bullet/Cl^-}$ [d]	1.76	1.81	2.1	2.16
$\phi^S - \phi^W$	0.202	−0.016	0.002	−0.009
k_S [e]	0.59	0.38	0.30	0.12
C [f]	0.95	1.00	1.03	1.13

[a] Energies in eV, potentials in V. [b] Standard free energies of transfer from water to the solvent S (from ref 20). [c] Standard free energy of solvation. [d] Standard potential of the subscript couple vs aq SCE.[10a] [e] Standard rate constant for the reduction of benzaldehyde in cm s^{-1}. [f] Coefficient in eq 21.

with

$$a = \sum_j |z_j| C_j^W u_j^W$$

$$b = \sum_j |z_j| \left[u_j^W (C_j^S - C_j^W) + C_j^W (u_j^S - u_j^W) \right]$$

$$c = \sum_j |z_j| (C_j^S - C_j^W)(u_j^S - u_j^W)$$

$$A = u_i^W \quad B = u_i^S - u_i^W$$

The ionic mobilities may as well be replaced by the limiting molar conductivities, Λ^∞. Applications of eq 1[23] thus lead to the results listed in Table 1.

In the case of DCE, the two solvents are immiscible. It can be assumed that KCl does not penetrate the organic solvent phase. Within this framework, the Donnan potential between the two phases may be obtained from the relationships describing the electrochemical equilibrium at the interface (see Supporting Information) leading to eq 2.

$$\phi^S - \phi^{IW} = \frac{\Delta^t G^{W\to S}_{A^-} - \Delta^t G^{W\to S}_{C^+}}{2} \qquad (2)$$

ϕ^S is, as before, the electrical potential in the organic solution. ϕ^{IW} is the electrical potential in the aqueous phase just outside the interface. It is, a priori, different from the potential in the bulk of the aqueous phase, ϕ^W, because of the junction potential between the interfacial and the bulk aqueous solutions which do not have the same ionic composition. $\Delta^t G^{W\to S}_{C^+}$ is the free energy of transfer, from water to DCE, of the cation of the supporting electrolyte in the DCE phase, that is, *n*-Bu_4N^+. $\Delta^t G^{W\to S}_{A^-}$ represents the same parameter for the anion. The energies are in electronvolts, and the electrical potentials, in volts. Assuming that $\Delta^t G^{W\to S}_{A^-}$ is the same for ClO_4^- and BF_4^- (0.1762 eV[20]) and taking $\Delta^t G^{W\to S}_{C^+} = -0.2280$ eV,[20] we find that $\phi^S - \phi^{IW} = 0.2021$ V.

The junction potential, $\phi^{IW} - \phi^W$, may then be estimated by the Henderson model, according to eq 3.

$$\phi^{IW} - \phi^W = -\frac{RT}{F} \frac{\sum_i \frac{|z_i|}{z_i} u_i (C_i^{IW} - C_i^W)}{\sum_i |z_i| u_i (C_i^{IW} - C_i^W)} \ln \frac{\sum_i |z_i| u_i C_i^{IW}}{\sum_i |z_i| u_i C_i^W} \qquad (3)$$

The interfacial concentrations of C^+ and A^- on the aqueous side are obtained from eq 4

$$\frac{RT}{F} \ln\left(\frac{C^{IW}_{C^+}}{C^S_{C^+}}\right) = \frac{RT}{F} \ln\left(\frac{C^{IW}_{A^-}}{C^S_{A^-}}\right) = \frac{\Delta^t G^{W\to S}_{C^+} + \Delta^t G^{W\to S}_{A^-}}{2} \qquad (4)$$

leading to $C^+_{IW} = A^-_{IW} = 0.0359$ M and, from eq 3, to $\phi^{IW} - \phi^W = 0.09$ mV, a perfectly negligible figure. In total, one thus obtains the figure reported in Table 1.

We may note that in the three polar solvents, the correction for the junction potential is small, thus making unimportant small defects in the model used. In contrast, the potential difference between the DCE and aqueous solutions is large, but it is a Donnan potential with a negligible contribution of an additional junction potential. Thus, despite its larger amplitude, the correction procedure appears reliable in the case of DCE, too.

Global Reorganization Energies from Brute Force Application of a Quadratic Activation−Driving Force Relationship. The conventional theory of dissociative electron transfer entails a quadratic relationship between the activation free energy, $\Delta G^\ddagger$, and the standard free energy of the reaction, ΔG°, as depicted by eq 5.[14]

$$\Delta G^\ddagger = \frac{\lambda}{4}\left(1 + \frac{\Delta G^\circ}{\lambda}\right)^2 \qquad (5)$$

The global reorganization energy, λ, contains a contribution pertaining to bond breaking, equal to the bond dissociation energy, D_R, and a solvent reorganization contribution, λ_0. Values of λ may be obtained by brute force application of eq 5 at the peak potential, E_p, that is, for a value of the standard free energy of reaction given by eq 6.

$$\Delta G^\circ = E_p - E^\circ_{RX/R^\bullet + X^-} \qquad (6)$$

In the fitting of the experimental data shown in Figure 2, the experimental values of $\Delta G^\ddagger$ were obtained, at each scan rate, from eq 7, in whose derivation the quadratic rate law is linearized around the peak (see Supporting Information).

$$\Delta G^\ddagger = \frac{RT}{F}\left[\ln\left(Z^{el}\sqrt{\frac{RT}{\alpha F \upsilon D}}\right) - 0.78\right] \qquad (7)$$

Because the value of α is needed in applying eq 7, we used an iteration procedure in which α is obtained from the differentiation of eq 5 in each loop.

The standard potentials for the reductive cleavage of the two compounds in the various solvents (Table 2) were derived from the previously determined values in DMF,[10a,b] taking into account the difference of the free energy of transfer from water to each solvent, $\Delta^t G^{W\to S}_{Cl^-}$, and the free energy of transfer from

(22) Henderson, P. *Z. Phys. Chem.* **1907**, *59*, 118.

(23)

	C^W	C^S	Λ^∞_W	Λ^∞_{DMF}	Λ^∞_{EtOH}	Λ^∞_{FA}
K^+	3.19	0	73.52	31.6	23.54	12.33
n-Bu_4N^+	0	0.1	19.5	26.9	19.4	6.54
Cl^-	3.19	0	76.34	53.8	21.85	17.46
BF_4^-	0	0.1	67.4	51.6	30.5	16.6

Λ s in $cm^2\ \Omega^{-1}\ mol^{-1}$ from ref 20. The values for BF_4^- to be the same as for ClO_4^-.

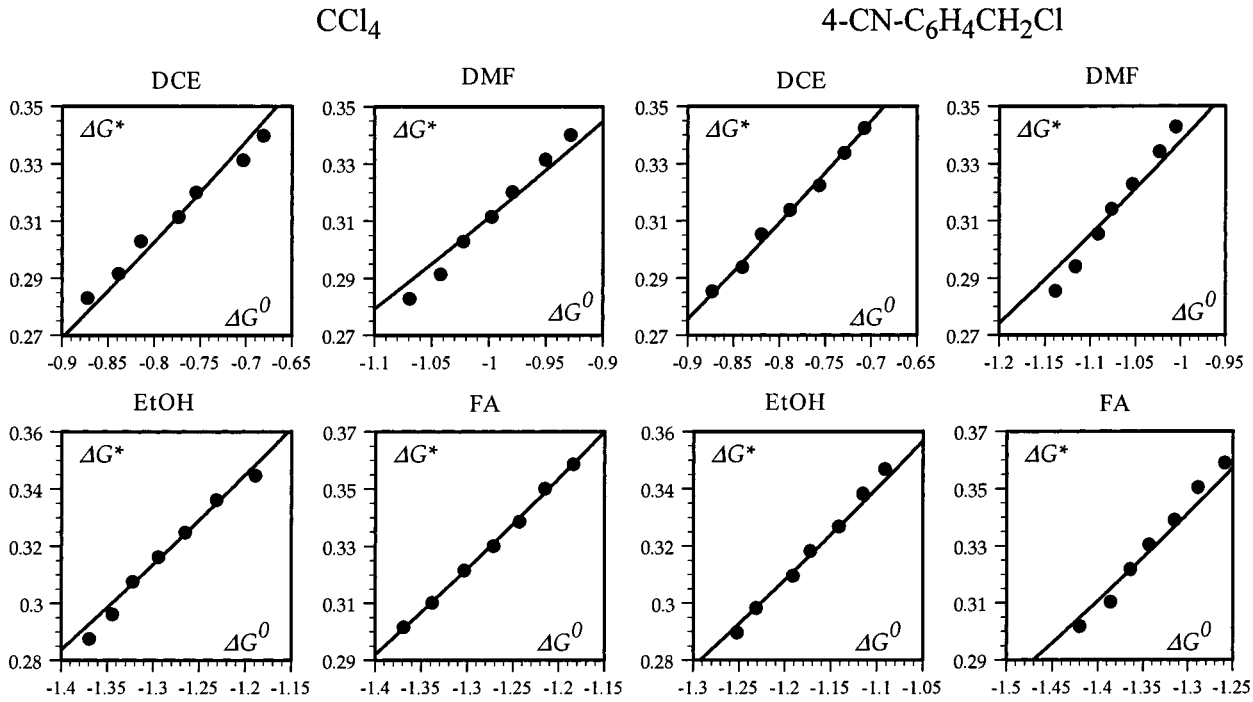

Figure 2. Fitting of the peak potential data (Figure 1) by brute force application of a quadratic activation−driving force relationship (eq 5).

Table 2.[a]

	DCE	DMF	EtOH	FA
CCl_4 ($D_R = 2.84$, $Z^{el} = 5.02 \times 10^3$ cm s^{-1})				
$D \times 10^6$ [b]	7.58	8.0	5.9	1.93
$E^\circ_{RX/R^\bullet+X^-}$ [c]	−0.696	−0.650	−0.360	−0.300
λ^d	2.56	2.9	3.35	3.39
λ_0^{app} [e]	−0.28	0.06	0.51	0.55
4−$CNC_6H_4CH_2Cl$ ($D_R = 2.82$, $Z^{el} = 5.05 \times 10^3$ cm s^{-1})				
$D \times 10^6$ [b]	6.34	6.69	4.93	1.61
$E^0_{RX/R^\bullet + X^-}$ [c]	−0.756	−0.71	−0.42	−0.36
λ^d	2.59	3.02	3.18	3.48
λ_0^{app} [e]	−0.23	0.20	0.36	0.66

[a] Energies in eV, potentials in V. [b] Diffusion coefficient in cm^2 s^{-1} from the application of the Stokes−Einstein equation. [c] Standard potential for the reductive cleavage reaction, in V vs aq SCE (see text). [d] Global reorganization energy from the application of eq 5. [e] Apparent solvent reorganization energy from the difference between λ and D_R (eq 8).

water to DMF, $\Delta^t G^{W\to DMF}_{Cl^-}$ (Table 1):

$$E^{\circ,S}_{RCl/R^\bullet + Cl^-} = E^{\circ,DMF}_{RCl/R^\bullet + Cl^-} + \Delta G^{tW\to DMF}_{Cl^-} - \Delta G^{tW\to S}_{Cl^-}$$

In the computation of ΔG° (eq 6), the values of the peak potential were corrected from the estimated values of the potential difference between the organic solution and the aqueous SCE (Table 1).

We may note incidentally that errors in the determination of the peak potential or of the standard potential do not have a large impact on the values of λ thus determined. The transmission of errors obeys the following equations (from differentiation of eq 5, keeping $\Delta G^\ddagger$ constant):

$$\frac{\partial\lambda}{\partial\Delta G^\circ} = -\frac{4\alpha}{1-\left(\frac{\Delta G^\circ}{\lambda}\right)^2}$$

where

$$\alpha = \frac{\partial\Delta G^\ddagger}{\partial\Delta G^\circ} = 0.5\left(1+\frac{\Delta G^\circ}{\lambda}\right)$$

is the transfer coefficient (symmetry factor), leading to a value of $\partial\lambda/\partial\Delta G^\circ$ on the order of 1.5. To illustrate this point, we may compare the value of λ obtained with and without correction of the junction potential. We find that the error is below 1%.

In the conventional theory of dissociative electron transfer, λ is the sum of two contributions featuring bond cleavage and solvent reorganization (eq 8).

$$\lambda = D_R + \lambda_0^{app} \qquad (8)$$

Because we know the first term, that is, the bond dissociation energy, we may estimate the apparent solvent reorganization energy, λ_0^{app}.

From the ensuing values of λ_0^{app} listed in Table 2, it is clear that they are much too small to represent solvent reorganization plausibly. This is obvious for DCE, where the values of λ_0^{app} are negative, but is also true for the other three more polar solvents. For example, the solvent reorganization energy accompanying the electrochemical electron transfer to anthracene in DMF is 0.6 eV.[24] The solvent reorganization energy for the two reactions discussed here is certainly larger because the charge develops on a smaller volume. We are thus led to conclude from these preliminary observations that the contribution of bond breaking to the dynamics of the reaction is certainly overestimated by the conventional model. Perusal of the values found for λ and λ_0^{app} (Table 2) also shows that the difference between the experimental data and the conventional model decreases as the solvation energy of Cl^- increases (from left to right in Table 2).

Model of Dissociative Electron Transfer That Takes the Formation of an Ion/Radical Pair into Account. One way of decreasing the contribution of bond breaking is to assume that there is a non-negligible attractive interaction between the ion

(24) Kojima, H.; Bard, A. J. *J. Am. Chem. Soc.* **1975**, *97*, 6317.

and the radical produced upon dissociative electron transfer. This assumption is also consistent with the solvent effect that we have noted previously, since the formation of an ion/radical pair facilitating the reductive cleavage reaction, because this effect is expected to be less and less effective as the free chloride ion is more and more stabilized by the solvent. As discussed elsewhere,[9f,10b,c] this improved model is based on Morse-type energy profiles for the reactant (eq 9) and product (eq 10).

$$G_R = D_R Y^2 + \lambda_0(Y)X^2 \tag{9}$$

$$G_P = \Delta G^\circ - D'_P + D_R\left(1 - \sqrt{\frac{D'_P}{D_R}} - Y\right)^2 + \lambda_0(Y)(1-X)^2 \tag{10}$$

where D'_P is the energy of the interaction between the ion and the radical. Y is a coordinate representing the stretching of the cleaving bond. It is defined by eq 11

$$Y = 1 - \exp[-\beta(y - y_{RX})] \tag{11}$$

with $\beta = \nu(2\pi^2\mu/D_R)^{1/2}$, y is the bond length, y_{RX} is the equilibrium value of y in the reactant system, ν is the frequency of the cleaving bond, and μ is the reduced mass. X is a fictitious charge borne by the molecule, whose value is between 0 and 1, serving as index for solvent reorganization. The solvent reorganization energy, λ_0, is indicated as being a function of the bond-stretching index, Y. This provision relates to the fact that the volume offered to solvation changes as the bond stretches. If, in a first stage, we neglect the variation of λ_0, we see that the decrease in the intrinsic barrier caused by the formation of the ion/radical pair simply amounts to replacing D_R with $(\sqrt{D_R} - \sqrt{D'_P})^2$ as results from eq 12, which has been obtained from the saddle point on the intersection of the two surfaces defined by eqs 9 and 10.

$$\Delta G^\ddagger \approx \frac{(\sqrt{D_R} - \sqrt{D'_P})^2 + \lambda_0}{4}\left[1 + \frac{\Delta G^\circ - D'_P}{(\sqrt{D_R} - \sqrt{D'_P})^2 + \lambda_0}\right]^2 \tag{12}$$

As illustrated by experimental examples in the next sections, small changes in D'_P result in large effects on the reaction dynamics, either large variations of the activation free energy at a given electrode potential or large shifts of the peak potential at a given scan rate.

For what regards the variation of λ_0 with the bond-stretching coordinate, a reasonable approximation is the linear variation depicted by eq 13[10b]

$$\lambda_0(Y) = (1-Y)\lambda_0^R + Y\lambda_0^P = \lambda_0^R + (\lambda_0^P - \lambda_0^R)Y \tag{13}$$

where λ_0^R is the solvent reorganization energy that corresponds to the charge being spread over the entire molecule as in the nuclear configuration of the reactant system, while λ_0^P corresponds to the charge located on the leaving anion as it is in the product system. Another, seemingly different, approach is as follows.[10a] The free energy profiles of the product system both in the gas phase and in the solvent may be represented approximately by Morse curves having the same repulsive term as the reactant Morse curve, as pictured in Figure 3. Thus, while curve b represents the y (or Y) dependent part of the product curve in the solvent (eq 12), curve a represents the y (or Y) dependent part of the product curve in the gas phase (eq 16),

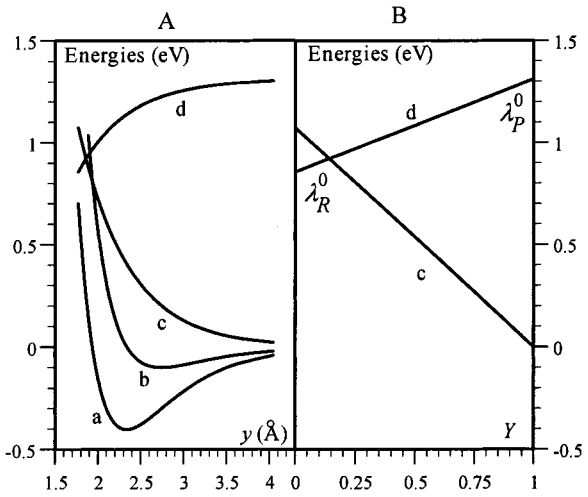

Figure 3. Example of energy profiles for R•, X^-. a. Potential energy in the gas phase. b. Potential energy in the solvent. c. Variation of the difference between the standard solvation free energy of the system and the standard solvation free energy of the free X^- ion. d. Solvent reorganization energy. The origin on the energy axis corresponds to infinite separation of the fragments. A. Variations with the length of the cleaving bond, y. B. Variations with the bond-stretching index Y defined by eq 13.

with the interaction energy in the ion/radical pair being much larger in the gas phase than in the solvent. The standard solvation free energy of the product system is thus the difference between the two curves, being thus represented by curve c in Figure 3. More exactly, what is represented by curve c is the difference between the standard solvation free energy of the system and the standard solvation free energy of the free X^- ion, $\Delta G^{\circ,\mathrm{solv}} = G^{\circ,\mathrm{solv}}_{R\bullet,X^-} - G^{\circ,\mathrm{solv}}_{X^-}$.

It may further be assumed that the solvent reorganization energy is proportional to the opposite of the standard solvation free energy of the system resulting in curve d in Figure 3, which depicts how this parameter increases during the course of the reaction. It is interesting to see that the solvent reorganization energy thus estimated is a linear function of the bond-stretching index Y varying from a value, λ_0^R, characterizing the configuration of the reactant system ($Y = 0$) to a value, λ_0^P, characterizing the configuration of the product system ($Y = 1$). This linear behavior, which was a priori assumed in the earlier treatment, is here a direct consequence of the representation of the free energy profiles of the product system in the gas phase and in the solvent by Morse curves having the same repulsive term. This shows that the two treatments are in fact equivalent.

Proceeding further to the derivation of the activation/driving force relationship, intersection of the two potential energy surfaces (eqs 9 and 10) and determination of the saddle point, taking due account of the variation of λ_0 with the coordinate Y (eq 13) finally leads to the following set of three equations characterizing the transition state (‡).

$$Y^\ddagger = \left(1 - \sqrt{\frac{D'_P}{D_R}}\right)X^\ddagger - \frac{\lambda_0^P - \lambda_0^R}{2D_R}X^\ddagger(1 - X^\ddagger) \tag{14}$$

$$\Delta G^\circ = D'_P + D_R\left(1 - \sqrt{\frac{D'_P}{D_R}}\right)\left[2Y^\ddagger - \left(1 - \sqrt{\frac{D'_P}{D_R}}\right)\right] + [\lambda_0^R + (\lambda_0^P - \lambda_0^R)Y^\ddagger](2X^\ddagger - 1) \tag{15}$$

$$\Delta G^{\ddagger} = D_R Y^{\ddagger 2} + [\lambda_0^R + (\lambda_0^P - \lambda_0^R) Y^{\ddagger}] X^{\ddagger 2} \quad (16)$$

Simultaneous resolution of the three equations allows the fitting of the experimental data and the determination of the interaction energy, D'_P. The transfer coefficient, α, to be used in an iterative procedure for fitting the experimental data (eq 7), is then simply given by eq 17.

$$\alpha = \partial \Delta G^{\ddagger} / \partial \Delta G^{\circ} = X^{\ddagger} \quad (17)$$

To proceed and treat the data summarized in Figure 1 according to the above model, we need a procedure for estimating λ_0^R and λ_0^P for each compound in each solvent. This is the purpose of the next section.

Estimation of the Solvent Reorganization Energy. The best strategy is to rely on experimental data pertaining to reversible systems in which solvent reorganization prevalently controls the dynamics of the charge-transfer reaction. In this connection, it has been shown,[1,14c] using previous experimental data,[24] that a satisfactory estimation of λ_0 in DMF is provided by eq 18

$$\lambda_0\,(\text{eV}) = \frac{3}{a\,(\text{Å})} \quad (18)$$

for the treatment of electrochemical rate data with no correction for the double layer effect, where a is the radius of the sphere equivalent to the molecule as can be derived from, for example, density data. We may thus obtain λ_0^R and λ_0^P in DMF by application of eq 18 using $a_{CCl_4} = 3.37$ Å, $a_{4-CNC_6H_4CH_2Cl} = 4.03$ Å, and $a_{Cl^-} = 1.81$ Å as reported in Table 3 (the radii are obtained from the molar mass and the density for neutral species and from crystallographic data for Cl^-).

For the other solvents, eq 19 may be used in place of eq 18 after determination of the coefficient C.

$$\lambda_0\,(\text{eV}) = \frac{3}{a\,(\text{Å})} C \quad (19)$$

C was derived from the variation of the standard rate constant for the electron transfer to benzaldehyde when passing from DMF to the solvent. At sufficiently high scan rates, the dimerization of the anion radical formed upon electron transfer to benzaldehyde does not interfere in the cyclic voltammetric response, which thus becomes chemically reversible. After careful correction of the ohmic drop, the difference between the anodic and cathodic peak potentials and its variation with the scan rate provide a measure of the standard rate constant, k_S (see Experimental Section). The k_S values are summarized in Table 1.

$$\lambda_{0,C_6H_5CHO}^{\text{solvent}} = \lambda_{0,C_6H_5CHO}^{\text{DMF}} + \frac{4RT}{F} \ln\left(\frac{k_S^{\text{DMF}}}{k_S^{\text{solvent}}}\right) \quad (20)$$

C is thus obtained from eq 21,

$$C = 1 + \frac{a_{C_6H_5CHO}}{3} \frac{4RT}{F} \ln\left(\frac{k_S^{\text{DMF}}}{k_S^{\text{solvent}}}\right) = 1 + 1.14 \frac{4RT}{F} \ln\left(\frac{k_S^{\text{DMF}}}{k_S^{\text{solvent}}}\right) \quad (21)$$

and its value in each solvent is reported in Table 1. The values of λ_0^R and λ_0^P (eq 19) ensue (Table 3).

Treatment of the Electrochemical Data. Determination of the Ion/Radical Interaction Energies. All the necessary ingredients are now available (Tables 1, 2, and 3) to treat the cyclic voltammetric data displayed in Figure 1. ΔG° is calculated by means of eq 6 from the peak potentials (Figure 1) and the values of $E^{\circ}_{RX/R\cdot+X^-}$ listed in Table 3. $\Delta G^{\ddagger}$ is obtained from eq 7 using the values of the parameters listed in Table 3. These experimental points are then fitted with eqs 14−16, leading to the results shown in Figure 4. The values of D'_P corresponding to the best fitting are listed in Table 3. The value of α, obtained from eq 17, is used to correct iteratively the experimental value of $\Delta G^{\ddagger}$.

Table 3. Characteristics of the Reductive Cleavage and Determination of the Ion/Radical Pair Stability[a]

	DCE	DMF	EtOH	FA
CCl_4 ($D_R = 2.84$, $Z^{el} = 5.02 \times 10^3$ cm s^{-1})				
$D \times 10^{6}$ [b]	7.58	8.0	5.9	1.93
$E^{\circ}_{RX/R\cdot+X^-}$ [c]	−0.696	−0.650	−0.360	−0.300
λ_0^R [d]	0.85	0.89	0.92	1.01
λ_0^P [e]	1.57	1.66	1.71	1.87
D'_P [f]	135 ± 13	88 ± 10	34 ± 7	40 ± 7
$\partial D'_P/\partial \Delta G^{\circ}$ [g]	0.36	0.30	0.20	0.21
$\partial D'_P/\partial \lambda^{\circ}$ [h]	0.18	0.15	0.10	0.11
4−$CNC_6H_4CH_2Cl$ ($D_R = 2.82$, $Z^{el} = 5.05 \times 10^3$ cm s^{-1})				
$D \times 10^{6}$ [b]	6.34	6.69	4.93	1.61
$E^{\circ}_{RX/R\cdot+X^-}$ [c]	−0.756	−0.71	−0.42	−0.36
λ_0^R [d]	0.71	0.74	0.77	0.84
λ_0^P [e]	1.57	1.66	1.71	1.87
D'_P [f]	121 ± 12	52 ± 8	36 ± 7	25 ± 6
$\partial D'_P/\partial \Delta G^{\circ}$ [g]	0.34	0.24	0.20	0.17
$\partial D'_P/\partial \lambda^{\circ}$ [h]	0.17	0.12	0.10	0.09

[a] Energies in eV, potentials in V. [b] Diffusion coefficient in cm^2 s^{-1} from the application of the Stokes−Einstein equation. [c] Standard potential for the reductive cleavage reaction, in V vs aq SCE. [d,e] Solvent reorganization energy in the reactant and product configuration, respectively. [f] Interaction energy in the ion/radical pair from the fitting (Figure 5) of the experimental data (Figure 1) with eqs 14−16. [g] Coefficient for the transmission of errors from ΔG° to D'_P. [h] Coefficient for the transmission of errors from λ_0 to D'_P.

Figure 4 also shows the values of the solvent reorganization energy in each case and its variation along the voltammetric wave as the transition state becomes more and more reactant-like.

The fact that even small variations of the interaction energy cause strong changes in the dynamics of the reaction is illustrated in the top diagrams of Figure 4 which represent the difference, ΔE_p, between the actual peak potential and the peak potential predicted to occur in the absence of interaction. The latter was obtained from the application of eq 5, making $\lambda = D + \lambda_0$ and taking for λ_0 the values shown in the middle diagrams of Figure 4. We see that even in the two protic solvents where the interaction energy is small (25−40 meV), its effect on the peak potential is quite large, of the order of 0.5 V.

There are two main sources of uncertainty in the determination of the interaction energy. One comes from errors on ΔG° caused by errors on E_p and on $E^{\circ}_{RX/R\cdot+X^-}$. The transmission of errors is given by the coefficient $\partial D'_P/\partial \Delta G^{\circ}$, which can be approximately estimated from application of eq 12, neglecting the quadratic term. Thus, $\partial D'_P/\partial \Delta G^{\circ} \approx 2/(\sqrt{D_R/D'_P} + 1)$, leading to the values reported in Table 3. The other source of uncertainty arises from the estimation of λ_0. $\partial D'_P/\partial \lambda^{\circ}$ may also be estimated by application of eq 12 with neglect of the quadratic term leading to $\partial D'_P/\partial \lambda^{\circ} \approx 1/(\sqrt{D_R/D'_P} + 1)$ and thus to the values reported in Table 3. The uncertainty in both E_p and on $E^{\circ}_{RX/R\cdot+X^-}$ may be estimated as ±10 mV in total, while the uncertainty in λ_0 is on the order of ±50 meV. Total uncertainty on the interaction energy thus ranges from 6 to 13 meV (see Table 3 and the error bars in Figure 5).

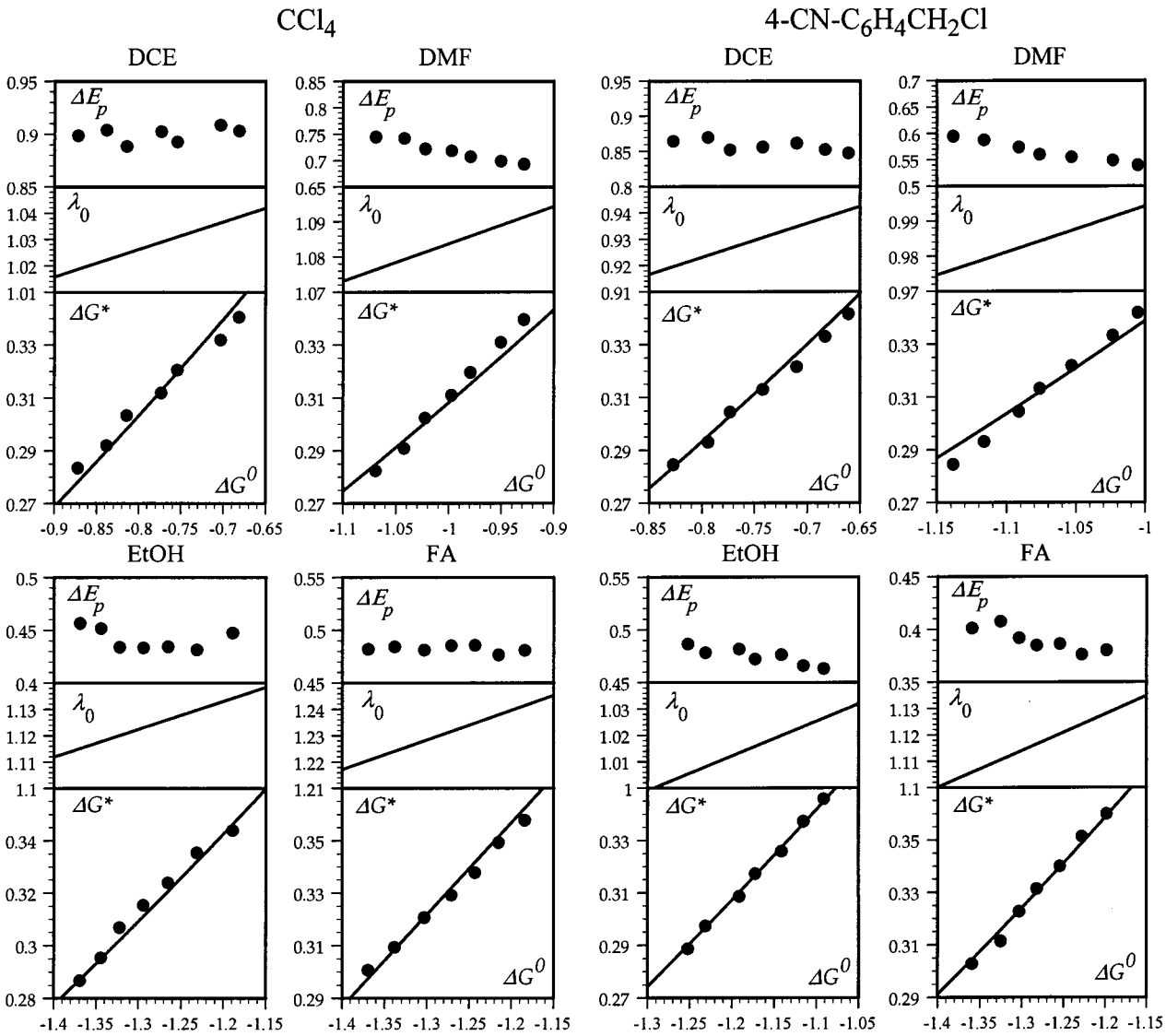

Figure 4. Fitting of the data in Figure 1 with eqs 14−16 with the D'_P values listed in Table 3. Energies in eV. ΔE_p (V) corresponds to the difference between the observed peak potential and the peak potential in absence of ion/radical interaction.

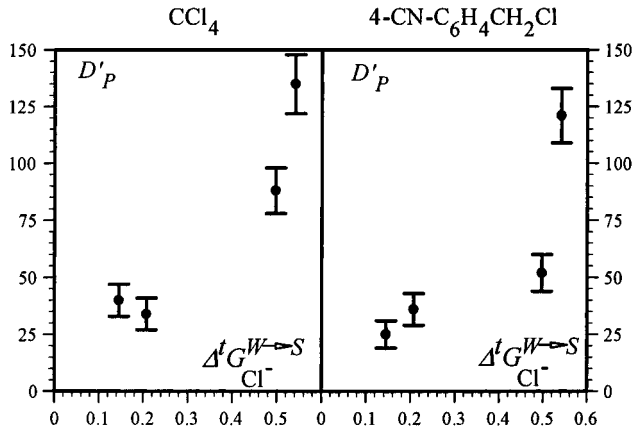

Figure 5. Plot of the interaction energies in the ion/radical pair against the standard free energies of transfer of Cl^- from water to the solvent. From left to right: FA, EtOH, DMF, DCE. Energies in eV on the horizontal axis and in meV on the vertical axis.

The interaction energies in the ion/radical pair thus obtained vary with the solvent in both the cases of CCl_4 and 4-$CNC_6H_4CH_2Cl$. As seen in Figure 5, D'_P is, roughly speaking, an increasing function of the standard free energies of transfer of Cl^- from water to each solvent, that is, of the solvation standard free energies of Cl^- in each solvent as well. There is no reason to expect a linear, or even a strictly monotonic, relationship between the interaction energy in the ion/radical pair and the standard free energies of Cl^-. It is true that the more negative the latter, the more stable the separated fragments, but a better solvation of Cl^- may also entail better solvation of the ion/radical pair as a whole. D'_P is the result of the difference between the solvation of the ion/radical pair and of the free fragments. Inspection of Figure 5 suggests the following remarks.

With both CCl_4 and 4-$CNC_6H_4CH_2Cl$, there is a non-negligible interaction between the fragments within the ion/radical pair, even in the polar solvents and even in the solvents, ethanol and formamide, that have the best ability to solvate chloride ion. The interaction is by far the biggest in 1,2-dichloroethane, which is both the least polar solvent and the least able to solvate Cl^-. Although the interaction is much less in the polar solvents, its strength is not the same in all three cases. The two protic solvents, ethanol and formamide, which are the most able to solvate Cl^-, give rise to similar interaction energies. However, *N*,*N*-dimethylformamide, which has a lesser

ability to solvate Cl^-, gives rise to a definitely stronger interaction than the two others.

Conclusions

Our quest for a dependence of fragment interactions in ion/radical pairs upon solvent has thus received a positive answer. The approximate correlation that is observed between the interaction energies in the ion/radical pair and the solvation free energies of the leaving anion, Cl^-, falls in line with the anticipation that the interaction should be essentially the ion-induced dipole interaction. At a finer detail level, several features are also worth noting. The interaction is maximal in 1,2-dichloroethane, which is both the least polar solvent and the least able to solvate Cl^-. The interaction is smaller in the polar solvents, albeit distinctly measurable. The two protic solvents, ethanol and formamide, which are the most able to solvate Cl^-, give rise to similar interaction energies. The interaction is definitely stronger in *N*,*N*-dimethylformamide, which has a lesser ability to solvate Cl^- than the two others.

Connecting these findings to the previous observations summed up in the Introduction leads to the unambiguous conclusion that significant attractive interactions may exist, depending on the nature of the ion and of the radical, within ion/radical pairs in the liquid phase even in polar solvents.

The work has also shown that application of the modified dissociative electron-transfer model to cyclic voltammetric data opens a route to the determination of the interaction energies with a reasonable accuracy.

Experimental Section

Chemicals. *N*,*N*-Dimethylformamide (Fluka, >99.5%, stored on molecular sieves under an argon atmosphere), ethanol (Normapur, 99.8%), formamide (Acros, >99.5%), and carbon tetrachloride (Acros, 99.8%) were used as received. Dichloroethane (Merck, >99%) was distilled before use. The supporting electrolyte *n*-Bu_4BF_4 (Fluka, puriss) was vacuum-dried before use.

4-Cyanobenzyl chloride was prepared from the corresponding bromide as follows. 4-Cyanobenzyl bromide (Aldrich, 99%) was dissolved in an acetone/dichloromethane (50/50) mixture in the presence of a 10-fold excess of tetraethylammonium chloride (Acros, 99%) and then refluxed for 1 h. After evaporation and addition of ether, the remaining salt precipitated, and the organic phase was filtered and evaporated. The resulting 4-cyanobenzyl chloride was recrystallized from a pentane/dichloromethane (60/40) mixture, leading to an 84% yield of pure compound. The structure was checked by elemental analysis and ^1H NMR.

Cyclic Voltammetry. The working electrode was a 3 mm diameter glassy carbon electrode disk (Tokai), carefully polished and ultrasonically rinsed in absolute ethanol before use. The counter electrode was a platinum wire, and the reference electrode, an aqueous SCE electrode. The potentiostat, equipped with positive feedback compensation and current measurer was the same as previously described.[25] All experiments have been carried out at 20 °C using a double-wall cell thermostated by circulation of water.

(25) Garreau, D.; Savéant, J.-M. *J. Electroanal. Chem.* **1972**, *35*, 309.

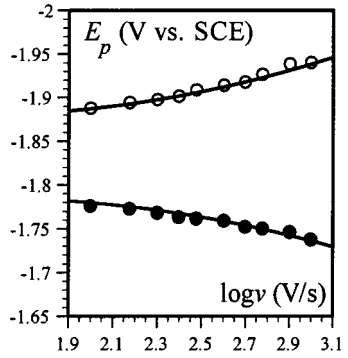

Figure 6. Cyclic voltammetry of benzaldehyde (1.18 mM) in DMF + 0.1 M *n*-Bu_4BF_4. Cathodic (○) and anodic (●) peak potentials as a function of the scan rate. $\Delta R_u = 35\ \Omega$; $C_d = 0.1\ \mu F$.

The raw values of the peak potentials were corrected for the ohmic drop that remained after in situ positive feedback compensation according to the following procedure. After determination of the residual uncompensated resistance, ΔR_u, and of the double layer capacitance, C_d,[25] the effect of the ohmic drop on the peak potential is simulated (Digisim) as a function of the scan rate for an irreversible electron-transfer reaction having the same values of α and D as the experimental system, with the same electrode surface area, the same C_d, and the same ΔR_u. We thus found that the ohmic drop $\delta E_p = 1.25\Delta R_u i_p - 0.096$ (in V). This equation is close to the same for the two compounds in all solvents and may thus be used to correct the residual ohmic drop appearing in the upper portion of the range of scan rates.

The standard rate constant, k_S, for the reduction of benzaldehyde was obtained from experiments where a hanging mercury drop was used as working electrode allowing scan rates up to 2500 V/s to be used, which proved necessary to reach chemical reversibility in FA. In all other solvents, chemical reversibility could be reached below 1000 V/s.[26] Typical peak potential data are shown in Figure 6. The value of k_S was derived from the simulation of the cyclic voltammograms with a transfer coefficient equal to 0.5 and a diffusion coefficient equal to 7.5×10^{-6}, 7.9×10^{-6}, 5.9×10^{-6}, and 1.9×10^{-6} $cm^2\ s^{-1}$ in DCE, DMF, EtOH, and FA, respectively. These values were obtained from the application of the Stokes−Einstein relationship,[27] that is, $D = kT/6\pi\eta a$ (k, Boltzmann constant; η, viscosity; a, radius = 3.4 Å), after checking that this approximation provides correct values on several examples using the peak currents of reversible and irreversible waves obtained with the compounds investigated in this work (and with ferrocene) in the four solvents.

Supporting Information Available: Derivation of eqs 1, 2, 4, 7, and 20. This material is available free of charge via the Internet at http://pubs.acs.org.

JA0117985

(26) (a) A detailed account of the cyclic voltammetry of benzaldehyde in ethanol is reported in ref 26b. (b) Andrieux, C. P.; Grzeszczuk, M.; Savéant, J.-M. *J. Am. Chem. Soc.* **1991**, *113*, 8811.

(27) Murov, L.; Carmichael, I.; Hug, L. *Handbook of Photochemistry*, 2nd Ed.; Dekker: New York, 1993; p 207.